

## 2.4 NONCLINICAL OVERVIEW

090177e1a39ef23a\Approved\Approved On: 23-May-2025 19:18 (GMT)

ema.europa.eu  
Data up to date as of 12 June 2025

## TABLE OF CONTENTS

LIST OF ABBREVIATIONS AND DEFINITION OF TERMS .....	4
2.4.1. OVERVIEW OF NONCLINICAL TESTING STRATEGY .....	6
Table 2.4.1-1. Nomenclature of the Vaccine Candidates .....	6
Table 2.4.1-2. Nonclinical Studies .....	8
2.4.2. PHARMACOLOGY .....	11
2.4.2.1. Primary Pharmacodynamics .....	11
2.4.2.1.1. Summary .....	11
2.4.2.1.2. BNT162b2, A Lipid Nanoparticle Encapsulated RNA Vaccine Encoding the SARS-CoV-2 P2 S as a Vaccine Antigen.....	12
Figure 2.4.2-1. Schematic of the Organization of the SARS-CoV-2 S Glycoprotein .....	13
2.4.2.1.3. Immunogenicity of BNT162b2 in Mice .....	13
2.4.2.1.4. Evaluation of BNT162b2 Immunogenicity and Protection Against SARS-CoV-2 Challenge in Rhesus Macaques.....	14
2.4.2.1.4.1. Immunogenicity in Rhesus Macaques .....	14
2.4.2.1.4.2. SARS-CoV-2 Challenge of BNT162b2 Immunized Nonhuman Primates .....	15
2.4.2.1.5. Immunogenicity Testing After Weekly Immunization of Rats in GLP Compliant Repeat Dose Toxicology Studies and a Developmental and Reproductive Toxicity Study...	15
2.4.2.1.6. Variant-Adapted Vaccine Immunogenicity Studies .....	16
Figure 2.4.2-2. Epidemiology Trajectories of SARS-CoV-2 JN.1 Sublineages .....	17
Figure 2.4.2-3. Global Prevalence Proportions of SARS-CoV-2 Variants .....	17
Figure 2.4.2-4. Antigenic Distance of Major SARS-CoV-2 Omicron JN.1 Variants/Subvariants Lineages Assessed in Vaccine Naïve Mice.....	18
2.4.2.1.6.1. DP.8.1 Variant-Adapted Vaccine .....	18
2.4.2.2. Secondary Pharmacodynamics .....	19
2.4.2.3. Safety Pharmacology .....	20
2.4.2.4. Pharmacodynamic Drug Interactions .....	20
2.4.2.5. Summary of Nonclinical Pharmacology Findings .....	20
2.4.3. PHARMACOKINETICS .....	21
2.4.3.1. Brief Summary .....	21
2.4.3.2. Methods of Analysis .....	22
2.4.3.3. Absorption .....	22
2.4.3.3.1. In Vitro Absorption .....	22
2.4.3.3.2. Single-Dose Pharmacokinetics .....	22

Table 2.4.3-1. PK of ALC-0315 and ALC-0159 in Wistar Han Rats After IV Administration of LNPs Containing Surrogate Luciferase mRNA at 1 mg/kg.....	22
Figure 2.4.3-1. Plasma and Liver Concentrations of ALC-0315 and ALC-0159 in Wistar Han Rats After IV Administration of LNPs Containing Surrogate Luciferase mRNA at 1 mg/kg.....	23
2.4.3.4. Distribution .....	23
Figure 2.4.3-2. Bioluminescence Emission in Balb/c Mice after IM Injection of an LNP Formulation of modRNA Encoding Luciferase.....	24
2.4.3.5. Metabolism .....	26
Figure 2.4.3-3. Proposed Biotransformation Pathway of ALC-0315 in Various Species .....	27
Figure 2.4.3-4. Proposed Biotransformation Pathway of ALC-0159 in Various Species .....	28
2.4.3.6. Excretion .....	28
2.4.3.7. Pharmacokinetic Drug Interactions .....	28
2.4.4. TOXICOLOGY .....	29
2.4.4.1. Brief Summary .....	29
Table 2.4.4-1. Overview of Toxicity Testing Program of BNT162 Vaccines Using modRNA-LNP Platform.....	29
2.4.4.2. Single-Dose Toxicity .....	30
2.4.4.3. Repeat-Dose Toxicity .....	30
2.4.4.4. Genotoxicity .....	31
2.4.4.5. Carcinogenicity .....	31
2.4.4.6. Reproductive and Developmental Toxicity .....	31
2.4.4.7. Local Tolerance .....	31
2.4.4.8. Other Toxicity Studies .....	31
2.4.4.8.1. Phototoxicity .....	31
2.4.4.8.2. Antigenicity .....	32
2.4.4.8.3. Immunotoxicity .....	32
2.4.4.8.4. Mechanistic Studies .....	32
2.4.4.8.5. Dependence .....	32
2.4.4.8.6. Studies on Metabolites .....	32
2.4.4.8.7. Studies on Impurities .....	32
2.4.4.8.8. Other Studies .....	32
2.4.4.9. Discussion of Findings .....	32
2.4.5. INTEGRATED OVERVIEW AND CONCLUSIONS .....	34
2.4.6. LIST OF LITERATURE REFERENCES .....	37

**LIST OF ABBREVIATIONS AND DEFINITION OF TERMS**

A:G	Albumin:globulin ratio
ACE2	Angiotensin-converting enzyme 2
ADME	Absorption, distribution, metabolism, excretion
ALC-0159	Proprietary PEG-lipid included as an excipient in the LNP formulation used in BNT162b2
ALC-0315	Proprietary amino-lipid included as an excipient in the LNP formulation used in BNT162b2
BAL	Bronchoalveolar lavage
BLI	Bioluminescence imaging
CBER	Center for Biologics Evaluation and Research
CD	Cluster of differentiation
COVID-19	Coronavirus Disease 2019
DART	Developmental and reproductive toxicity
dLIA	Direct Luminex immunoassay
DNA	Deoxyribonucleic acid
DSPC	1,2-distearoyl-sn-glycero-3-phosphocholine
ELISA	Enzyme-linked immunosorbent assay
F0	Parental generation administered vaccine
F1	First generation offspring of F0 generation
GD	Gestation day
GFP	Green fluorescent protein
GGT	Gamma-glutamyl transferase
GLP	Good Laboratory Practice
GMT	Geometric mean titer
H	Human (in metabolite scheme)
HCS	Human convalescent sera
[ <sup>3</sup> H]-CHE	Radiolabeled [Cholesteryl-1,2- <sup>3</sup> H(N)]-Cholesteryl Hexadecyl Ether
HPD	Hours post dose
IFN	Interferon
IgG	Immunoglobulin G
IHC	Immunohistochemistry
IL	Interleukin
IM	Intramuscular(ly)
ISH	In situ hybridization
IV	Intravenous(ly)
LC/MS	Liquid chromatography-tandem mass spectrometry
LD	Lactation day
LNP	Lipid-nanoparticle
Mk	Monkey (in metabolite scheme)
Mo	Mouse (in metabolite scheme)
M0	Prior to mating phase
modRNA	Nucleoside-modified mRNA
mRNA	Messenger RNA
NA	Not applicable
OECD	Organisation for Economic Co-operation and Development
P2 S	Spike protein P2 mutant
PEG	Polyethylene glycol
PK	Pharmacokinetics
PLT	Platelet
PND	Postnatal day
pVNT	Pseudovirus neutralization test

**LIST OF ABBREVIATIONS AND DEFINITION OF TERMS**

QW	Once weekly
R	Rat (in metabolite scheme)
RBC	Red blood cell
RBD	Receptor binding domain
RDW	Red cell distribution width
RETIC	Reticulocyte
RNA	Ribonucleic acid
RT-qPCR	Reverse transcription-quantitative polymerase chain reaction
S	SARS-CoV-2 spike glycoprotein
S1	S1 domain of the SARS-CoV-2 spike glycoprotein
S2	S2 domain of the SARS-CoV-2 spike glycoprotein
S9	Supernatant fraction obtained from liver homogenate by centrifuging at 9000 g
SARS-CoV-2	Severe acute respiratory syndrome coronavirus 2; coronavirus causing COVID-19
Tfh	T follicular helper cell
Th1	Type 1 T helper cells
Th2	Type 2 T helper cells
TK	Toxicokinetic
TNF	Tumor necrosis factor
VOC	Variant of concern
WBC	White blood cell
WHO	World Health Organization

### 2.4.1. OVERVIEW OF NONCLINICAL TESTING STRATEGY

BNT162b2 (BioNTech code number BNT162, Pfizer code number PF-07302048) is a vaccine intended to prevent COVID-19, which is caused by SARS-CoV-2. BNT162b2 is a nucleoside modified mRNA (modRNA) expressing full-length S with two proline mutations (P2) to lock the transmembrane protein in an antigenically optimal prefusion conformation (Pallesen et al, 2017; Wrapp et al, 2020). The vaccine is formulated in lipid nanoparticles (LNPs). The LNP is composed of 4 lipids: ALC-0315, ALC-0159, DSPC, and cholesterol. Other excipients in the formulation include sucrose, tromethamine (Tris base), and Tris hydrochloride.

Efficacy of the original vaccine was demonstrated in Phase 3 clinical evaluation, with improved immunogenicity against variants of concern demonstrated with subsequent variant-modified vaccines. The variant-modified vaccines are described in the table below (Table 2.4.1-1).

**Table 2.4.1-1. Nomenclature of the Vaccine Candidates**

Product Code	RNA Platform	Description/Translated Protein
BNT162b2	modRNA	P2 S (Original)
BNT162b2	modRNA	P2 S (Omicron BA.4/BA.5)
BNT162b2	modRNA	P2 S (Omicron XBB.1.5)
BNT162b2	modRNA	P2 S (Omicron JN.1)
BNT162b2	modRNA	P2 S (Omicron KP.2)
<b>BNT162b2</b>	<b>modRNA</b>	<b>P2 S (Omicron LP.8.1)</b>

With the continuing evolution of SARS-CoV-2 variants and subvariants, variant-modified vaccines based on BNT162b2 that contain variant-specific mutations have also been evaluated in nonclinical immunogenicity studies (Section 2.4.2.1.6.1).

The primary pharmacology, distribution, metabolism, and safety of BNT162b2 were evaluated in nonclinical pharmacology, pharmacokinetic, and toxicity studies in vitro and in vivo (Table 2.4.1-2).

Immunogenicity of BNT162b2 was evaluated in mice (Section 2.4.2.1.3), rats (Section 2.4.2.1.5) and nonhuman primates (Section 2.4.2.1.4). Immunogenicity of variant-modified vaccines was evaluated in mice (Section 2.4.2.1.6). For assessment of serum antibody responses in mice and rats, S1 and RBD-binding IgG responses were tested by an ELISA. Functional antibody responses were tested by a SARS-CoV-2 pseudotyped virus neutralization test (pVNT) or a recombinant SARS-CoV-2 live virus neutralization assay. In nonhuman primate studies, S1-binding IgG responses were tested in a direct Luminex-based immunoassay (dLIA) and functional antibody responses were assessed in a SARS-CoV-2 neutralization assay. S-specific T cell responses and the Th1/Th2 profile were assessed on splenocytes in mouse and nonhuman primate studies by intracellular cytokine staining flow cytometry-based analysis and an IFN $\gamma$  ELISpot assay.

A SARS-CoV-2 challenge study in BNT162b2-immunized nonhuman primates was also conducted to assess protection against infection and to demonstrate lack of disease enhancement ([Section 2.4.2.1.4.2](#)).

Platform properties that support BNT162b2 were initially demonstrated with non-SARS-CoV-2 antigens. Non-GLP in vivo testing of LNP-formulated modRNA encoding luciferase or GFP examined biodistribution in mice and rats after IM injection ([Section 2.4.3.4](#)) and the PK of the two novel excipients in the LNP formulation, ALC-0315 and ALC-0159, in Wistar Han rats ([Section 2.4.3.3](#)). The biodistribution of BNT162b2 was assessed using luciferase or GFP mRNA and protein expression as surrogate reporters or radiolabeled [<sup>3</sup>H]CHE-, a nonexchangeable, nonmetabolizable lipid marker. Biodistribution of the BNT162b2 mRNA and its translation to spike protein was then evaluated in mice ([Section 2.4.3.4](#)). In addition, the metabolism of ALC-0315 and ALC-0159 was evaluated in mouse, rat, monkey, and human blood, liver microsomes, S9 fractions, and hepatocytes and in vivo in rat plasma, urine, feces, and liver samples from the PK study ([Table 2.4.1-2](#); [Section 2.4.3.5](#)).

BNT162b2 has been studied in GLP-compliant repeat-dose toxicity studies in rats ([Table 2.4.1-2](#)). Two GLP repeat-dose toxicity studies for BNT162b2 have been completed. The study designs are described in [Section 2.4.4](#) and are based on WHO guidelines for vaccine development ([WHO, 2005](#)). A DART study with BNT162b2 in rats has also been completed. No additional toxicity studies are planned for BNT162b2 variant or subvariants.

IM administration was chosen for the toxicity studies as this is the intended route of administration. Rats were chosen for toxicity assessments as they are a commonly used animal species for the evaluation of toxicity, and they mount an antigen-specific immune response to vaccination with BNT162b2.

The design of the nonclinical repeat-dose toxicity studies was consistent with the WHO Guidelines on Nonclinical Evaluation of Vaccines, the EMA Note for Guidance on Preclinical Pharmacological and Toxicological Testing of Vaccines, and Japan guidance on the nonclinical safety assessment of vaccines. In addition, the 2020 CBER guidance on “Development and Licensure of Vaccines to Prevent COVID-19” ([US FDA, 2020](#)) was considered when assembling the nonclinical safety licensure package as well as feedback from regulatory agencies. All GLP-compliant studies were conducted in accordance with Good Laboratory Practice for Nonclinical Laboratory Studies, Code of US Federal Regulations (21 CFR Part 58), in an OECD Mutual Acceptance of Data member state. All nonclinical studies described herein were conducted by or for Pfizer Inc or BioNTech Pharmaceuticals GmbH. The location of records for inspection is included in each final study report.

**Table 2.4.1-2. Nonclinical Studies**

Study Number	Study Type	Species/ Test System	Test Item	Dose [RNA]	Cross reference
<b>Pharmacology - BNT162b2 studies</b>					
VR-VTR-10741	In vitro protein expression	Cell culture	BNT162b2	Varied	<a href="#">Section 2.6.2.4</a>
R-20-0085	In vivo immunogenicity	BALB/c mice	BNT162b2	0.2, 1, 5 µg	<a href="#">Section 2.6.2.5</a>
VR-VTR-10944	In vivo immunogenicity	BALB/c mice	BNT162b2 Omicron BA.1 variant-modified vaccine	0.5 µg	<a href="#">Section 2.6.2.6</a>
VR-VTR-10976	In vivo immunogenicity	BALB/c mice	BNT162b2 Omicron BA.4/BA.5 variant-modified vaccine	0.5 µg	<a href="#">Section 2.6.2.6</a>
VR-VTR-11122	In vivo immunogenicity	BALB/c mice	BNT162b2 Omicron (XBB.1.5) variant-modified vaccines	0.5 µg	<a href="#">Section 2.6.2.7</a>
VR-VTR-11123	In vivo immunogenicity	BALB/c mice	BNT162b2 Omicron (XBB.1.5) variant-modified vaccines	0.5 µg	<a href="#">Section 2.6.2.7</a>
VR-VTR-11341	In vivo immunogenicity	BALB/c mice	BNT162b2 Omicron (JN.1 and KP.2) variant-modified vaccine	0.5 µg	<a href="#">Section 2.4.2.1.6.1</a> <a href="#">Section 2.6.2.8.2</a>
VR-VTR-11342	In vivo immunogenicity	BALB/c mice	BNT162b2 Omicron (JN.1 and KP.2) variant-modified vaccine	0.5 µg	<a href="#">Section 2.4.2.1.6.1</a> <a href="#">Section 2.6.2.8.1</a>
VR-VTR-11311	In vivo immunogenicity	BALB/c mice	BNT162b2 Omicron (JN.1) variant-modified vaccine	0.5 µg	<a href="#">Section 2.6.2.9.2</a> <a href="#">Section 2.6.2.9.2.1</a> <a href="#">Section 2.6.2.9.2.2</a>
VR-VTR-11313	In vivo immunogenicity	BALB/c mice	BNT162b2 Omicron (JN.1) variant-modified vaccine	0.5 µg	<a href="#">Section 2.6.2.9.1</a> <a href="#">Section 2.6.2.9.1.1</a> <a href="#">Section 2.6.2.9.1.2</a>
VR-VTR-11466	In vivo immunogenicity	BALB/c mice	BNT162b2 Omicron (KP.2 and LP.8.1) variant-modified vaccine	0.5 µg	<a href="#">Section 2.4.2.1.6</a> <a href="#">Section 2.4.2.1.6.1</a> <a href="#">Section 2.6.2.10.1</a> <a href="#">Section 2.6.2.10.1.2</a>
VR-VTR-11467	In vivo immunogenicity	BALB/c mice	BNT162b2 Omicron (KP.2 and LP.8.1) variant-modified vaccine	0.5 µg	<a href="#">Section 2.4.2.1.6.1</a> <a href="#">Section 2.6.2.10.2</a>



**Table 2.4.1-2. Nonclinical Studies - Continued**

Study Number	Study Type	Species/ Test System	Test Item	Dose [RNA]	Cross reference
VR-VTR-10671	In vivo immunogenicity and SARS-CoV-2 challenge	Rhesus macaques	BNT162b2	30 and 100µg	<a href="#">Section 2.4.2.1.4.2</a> <a href="#">Section 2.6.2.11</a> <a href="#">Section 2.6.2.11.2</a> <a href="#">Section 2.6.2.16</a>
<b>ADME</b>					
PF-07302048 _06Jul20_072424	PK of ALC-0315 and ALC-0159	Wistar Han Rats	modRNA encoding luciferase formulated in LNP comparable to BNT162b2	1 mg/kg	<a href="#">Section 2.4.3.3</a>
R-20-0072	In vivo distribution	BALB/c mice	modRNA encoding luciferase formulated in LNP comparable to BNT162b2	2 µg	<a href="#">Section 2.4.3.4</a>
185350	In vivo distribution	Wistar Han Rats	modRNA encoding luciferase formulated in LNP comparable to BNT162b2 with trace amounts of [ <sup>3</sup> H]-CHE as non-diffusible label	50 µg	Section 2.4.3.4
R-23-0355	In vivo distribution	BALB/c mice	modRNA encoding luciferase formulated in LNP comparable to BNT162b2	0.2 and 1 µg	Section 2.4.3.4
R-23-0475	In vivo distribution	BALB/cJ mice	BNT162b2 modRNA formulated in LNP	1 µg	Section 2.4.3.4
22GR161	In vivo cellular distribution and protein expression	CD-1 mice	modRNA encoding GFP formulated in LNP	2 µg	Section 2.4.3.4

**Table 2.4.1-2. Nonclinical Studies - Continued**

Study Number	Study Type	Species/ Test System	Test Item	Dose [RNA]	Cross reference
01049-20008	In vitro metabolism	CD-1/ICR mouse, Wistar Han and/or Sprague Dawley rat, cynomolgus monkey and human liver microsomes, S9 fraction, hepatocytes	ALC-0315	NA	<a href="#">Section 2.4.3.5</a>
01049-20009					
01049-20010					
01049-20020			ALC-0159	NA	
01049-20021					
01049-20022					
PF-07302048 _05Aug20_04372 5	In vitro and in vivo metabolism	Blood, liver S9 fractions and hepatocytes from CD-1 mouse, Wistar Han rat, cynomolgus monkey and human. In vivo samples from Wistar Han rat plasma, urine, feces, and liver	In vitro: ALC-0315 and ALC-0159  In vivo: modRNA encoding luciferase formulated in LNP comparable to BNT162b2	1 mg/kg modRNA (in vivo samples)	Section 2.4.3.5
<b>Toxicology – BNT162b2 studies</b>					
38166	Repeat-dose toxicity	Wistar Han Rats	BNT162b2	100 µg	<a href="#">Section 2.4.4.3</a>
20GR142	Repeat-dose toxicity	Wistar Han Rats	BNT162b2	30 µg	Section 2.4.4.3
20256434	Development and Reproductive Toxicity	Wistar Han Rats	BNT162b2	30 µg	<a href="#">Section 2.4.4.6</a>

## 2.4.2. PHARMACOLOGY

### 2.4.2.1. Primary Pharmacodynamics

#### 2.4.2.1.1. Summary

BNT162b2 (BioNTech code number BNT162, Pfizer code number PF-07302048) is a nucleoside-modified mRNA (modRNA) vaccine that encodes the SARS-CoV-2 full-length spike glycoprotein (S). The glycoprotein encoded by BNT162b2 includes two amino acid substitutions to proline (P2 S) locking the transmembrane protein in an antigenically optimal prefusion conformation (Wrapp et al, 2020; Pallesen et al, 2017). The mRNA is formulated with functional and structural lipids, which protect the RNA from degradation and enable transfection of the RNA into host cells after IM injection. S is a major target of virus neutralizing antibodies and is a key antigen for vaccine development. The well-resolved trimeric prefusion structure and the high affinity binding to ACE2 and human neutralizing antibodies demonstrate that the recombinant P2 S authentically presents the ACE2 binding site and other epitopes targeted by many SARS-CoV-2 neutralizing antibodies.

In vitro and in vivo studies in mice and nonhuman primates demonstrate the mechanism of action for this RNA-based vaccine, which is to encode SARS-CoV-2 S that is expressed by host cells and subsequently induces an immune response that is characterized by both a strong neutralizing antibody response and Th1-type CD4<sup>+</sup> and an IFN $\gamma$ <sup>+</sup> CD8<sup>+</sup> T cell response. BNT162b2 immunization demonstrated potent immunogenicity in mice and protected rhesus macaques from infectious SARS-CoV-2 challenge, with reduced detection of viral RNA in vaccine-immunized animals compared to saline-immunized animals and with no evidence of clinical exacerbation.

As new variants of concern (VOC) and their subvariants have emerged that are more transmissible and antigenically distinct from the original ancestral strain and last year's KP.2 candidate, variant-adapted vaccines containing variant-specific mutations applied to BNT162b2 have been evaluated as a primary series in naïve mice or as an updated dose to mice that were vaccine-experienced.

Prior preclinical data that supported the approval of the BNT162b2 monovalent (KP.2) vaccine in 2024 had shown that the KP.2-adapted vaccine elicited robust neutralizing antibody responses against the vaccine strain-matched variant and related variants (eg, JN.1, KP.3) that were 3-to-7-fold higher than responses elicited against the same subvariant by the comparator BNT162b2 XBB.1.5 vaccine in vaccine-experienced mice (VR-VTR-11342). Following a 2-dose primary series in naïve mice, responses with the BNT162b2 KP.2 vaccine were more than 10-fold higher than the BNT162b2 XBB.1.5 vaccine (VR-VTR-11341).

In the most recent evaluation, a BNT162b2 monovalent (LP.8.1) vaccine was evaluated either as a fourth dose in mice that had been vaccinated with 2 doses of BNT162b2 (Original) and 1 dose of bivalent BNT162b2 (Original + BA.4/5), or as a primary 2-dose series. In the current filing, the monovalent BNT162b2 LP.8.1 vaccine, administered as a fourth dose, elicited, 1.8-to-4-fold higher neutralizing responses against the LP.8.1 compared to the BNT162b2 KP.2 vaccine ([VR-VTR-11466](#)).

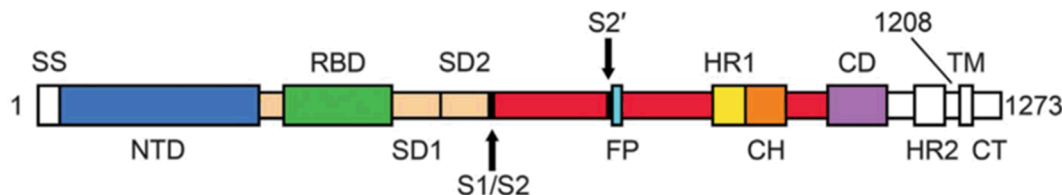
The monovalent BNT162b2 LP.8.1 vaccine given as a 2-dose primary series in naïve mice elicited neutralizing responses against the homologous JN.1 lineage and related sublineages that were between 2-to-7.7-fold higher than that elicited by the monovalent BNT162b2 KP.2 vaccine, demonstrating the notable antigenic distance between LP.8.1 and KP.2, and the clear benefit of a more closely strain-matched vaccine to elicit the relevant immune responses ([VR-VTR-11467](#)).

#### **2.4.2.1.2. BNT162b2, A Lipid Nanoparticle Encapsulated RNA Vaccine Encoding the SARS-CoV-2 P2 S as a Vaccine Antigen**

BNT162b2 is based on a nucleoside-modified mRNA (modRNA) platform technology. Vaccination with modRNA formulated in LNPs is characterized by strong expansion of Th1-skewed antigen-specific T follicular helper (Tfh) cells, which stimulate and expand germinal center B cells, thereby resulting in particularly strong, long-lived, high-affinity antibody responses ([Sahin et al, 2014](#); [Pardi et al, 2018](#)). ModRNA vaccine candidates against other infectious diseases induce strong antibody responses that prime and expand multifunctional CD4<sup>+</sup> and CD8<sup>+</sup> T cells ([Pardi et al, 2017](#); [Pardi et al, 2018](#)).

SARS-CoV-2 S is a large, trimeric glycoprotein that exists predominantly in a prefusion conformation on the virion ([Ke et al, 2020](#)). It is cleaved by furin into an N-terminal S1 and a C-terminal S2 fragment. S attaches to the host cell receptor, ACE2, by its receptor binding domain, which is contained in the S1 furin cleavage fragment. Spontaneously and during cell entry, the S1 fragment dissociates, and the S2 fragment undergoes a fold-back rearrangement to the post-fusion conformation in a process that facilitates fusion of viral and host cell membranes. S is the main target of virus neutralizing antibodies ([Zakhartchouk et al, 2007](#); [Yong et al, 2019](#)). Most of the antibodies with SARS-CoV-2 neutralizing activity are directed against the RBD ([Jiang et al, 2020](#); [Zost et al, 2020](#)).

**Figure 2.4.2-1. Schematic of the Organization of the SARS-CoV-2 S Glycoprotein**



The S1 furin cleavage fragment includes the signal sequence (SS), the N terminal domain (NTD), the receptor binding domain (RBD, which binds the human cellular receptor, ACE2), subdomain 1 (SD1), and subdomain 2 (SD2). The furin cleavage site (S1/S2) separates S1 from the S2 fragment, which contains the S2 protease cleavage site (S2') followed by a fusion peptide (FP), heptad repeats (HR1 and HR2), a central helix (CH) domain, the connector domain (CD), the transmembrane domain (TM) and a cytoplasmic tail (CT).

Source: modified from [Wrapp et al, 2020](#).

BNT162b2 encodes a full-length P2 S transmembrane protein that contains two consecutive prolines introduced at amino acid positions 986 and 987, between the central helix (CH) and heptad repeat 1 (HR1) (Figure 2.4.2-1) (Wrapp et al, 2020; [Pallesen et al, 2017](#)).

The RNA-expressed P2 S is membrane bound and elicits a potent humoral neutralizing antibody response and Th1-type CD4<sup>+</sup> and CD8<sup>+</sup> cellular response to block virus infection and kill virus-infected cells, respectively.

Efficient in vitro expression of the P2 S protein was demonstrated following in vitro transfection of cells with BNT162b2 RNA drug substance and BNT162b2 drug product. Electron cryomicroscopy analysis of purified recombinant P2 S, expressed from DNA encoding the same S amino acid sequence as BNT162b2 RNA (except for the addition of a C-terminal tag for protein purification) revealed high similarity to previously reported structures ([Cai et al, 2020](#)). The well-resolved trimeric prefusion structure and the high affinity binding to ACE2 and human neutralizing antibodies demonstrate that the recombinant full-length P2 S protein authentically presents the ACE2 binding site.

#### 2.4.2.1.3. Immunogenicity of BNT162b2 in Mice

BNT162b2 was highly immunogenic in mice with strong antigen-binding IgG and high titer neutralizing antibody responses together with a Th1-phenotype CD4<sup>+</sup> response as well as an IFN $\gamma$ , IL-2<sup>+</sup> CD8<sup>+</sup> T cell response after a single immunization. Total IgG ELISA results indicated the vaccine induced a strong, dose-dependent S1 and RBD specific IgG and elicited high neutralizing titers in a pseudotyped virus neutralization assay.

Stimulation of fresh splenocytes, collected 28 days after immunization, with an S protein specific overlapping peptide pool demonstrated robust CD4<sup>+</sup> and CD8<sup>+</sup> T cell IFN $\gamma$  responses and a Th1-dominant profile was demonstrated in quantification of cytokines (IL-2 and IFN $\gamma$ ) in the corresponding culture supernatants.

In summary, BNT162b2 induced a strong, neutralizing antibody response. CD4<sup>+</sup> and CD8<sup>+</sup> T cell responses were detectable 12 and 28 days after one immunization and exhibited a Th1 dominant T cell response characteristic of RNA-based vaccines.

#### **2.4.2.1.4. Evaluation of BNT162b2 Immunogenicity and Protection Against SARS-CoV-2 Challenge in Rhesus Macaques**

BNT162b2 was assessed for immunogenicity and for protection against an infectious SARS-CoV-2 challenge in rhesus macaques. SARS-CoV-2 infection in humans manifests as both asymptomatic infection and as the disease COVID-19, with diverse signs, symptoms, and levels of severity. Based on published reports, SARS-CoV-2 challenged rhesus macaques develop an acute, transient infection in the upper and lower respiratory tract and have evidence of viral replication in the gastrointestinal tract, similar to humans (Zou et al, 2020; Kim et al, 2020). Varying degrees of pulmonary inflammation, primarily at the peak of infection at approximately Day 2-to-4 post-challenge, have been reported in the literature (Munster et al, 2020). The human and rhesus ACE2 receptor have 100% amino acid identity at the critical binding residues, which may account for the fidelity of this SARS-CoV-2 animal model (Singh et al, 2021).

##### **2.4.2.1.4.1. Immunogenicity in Rhesus Macaques**

Rhesus macaques immunized IM with 30 µg or 100 µg of BNT162b2 on Days 0 and 21 had readily detectable S1-binding IgG and SARS-CoV-2 neutralizing titers (NT50) as early as 14 days after a single immunization, with substantial increases following the second immunization. On Day 28, 7 days after Dose 2 at the 30 µg dose level, the neutralizing geometric mean titer (GMT) reached 8-fold the GMT of a 38-member panel of human convalescent sera (HCS); at the 100 µg dose level, the neutralizing GMT was 18-fold the HCS GMT. The HCS sera were drawn from SARS-CoV-2 infected individuals 18 to 83 years of age, at least 14 days after PCR-confirmed diagnosis and at a time when individuals were asymptomatic. The HCS panel provides a currently accessible benchmark to judge the quality of the humoral immune response to the vaccine. A decline of both, S1-binding IgG levels and neutralizing titers, was observed out to the latest measured time point (Day 56) but remained above the neutralizing GMT and the S1-binding geometric mean concentration (GMC) of the HCS.

As seen following mouse immunization, strong S-specific Th1-dominant IFNγ<sup>+</sup> T cell responses were detected in all immunized rhesus macaques. By intracellular cytokine staining analysis, there was a dose-dependent increase in S-specific CD4<sup>+</sup> T cell responses with a strong Th1-bias evidenced by high frequency of IFNγ<sup>+</sup>, IL-2<sup>+</sup>, or TNF-α<sup>+</sup> cells. Notably, CD8<sup>+</sup> T cell responses were also detectable in BNT162b2-immunized animals.



#### 2.4.2.1.4.2. SARS-CoV-2 Challenge of BNT162b2 Immunized Nonhuman Primates

Groups of 2-4 year old male rhesus macaques that had received two IM immunizations with 100 µg BNT162b2 (n=6) or saline (control; n=3) 21 days apart were challenged 55 days after the second immunization with  $1.05 \times 10^6$  plaque forming units of SARS-CoV-2 (strain USA-WA1/2020), split equally between the intranasal (IN) and intratracheal (IT) routes, as previously described (Singh et al, 2021) (VR-VTR-10671). SARS-CoV-2 RNA was measured by reverse transcription-quantitative polymerase chain reaction (RT-qPCR) in bronchoalveolar lavage fluid, nasal swabs, and oropharyngeal swabs. The difference in viral RNA detection in BAL fluid between BNT162b2-immunised and control-immunised rhesus macaques after challenge is highly statistically significant (by a nonparametric test,  $p=0.0014$ ). None of the challenged animals showed clinical signs of significant illness, indicating that the 2-4 years old male rhesus challenge model is primarily an infection model for SARS-CoV-2, not a COVID-19 disease model. No radiographic or histological evidence of vaccine-elicited enhanced disease was observed. In summary, BNT162b2 provided complete protection from the presence of detectable viral RNA in the lungs compared to the saline control with no evidence of vaccine-elicited disease enhancement.

#### 2.4.2.1.5. Immunogenicity Testing After Weekly Immunization of Rats in GLP Compliant Repeat Dose Toxicology Studies and a Developmental and Reproductive Toxicity Study

The nonclinical safety data package consists of two GLP-compliant repeat-dose rat toxicity studies and a DART study, in which BNT162b2 was evaluated (Section 2.4.4).

In all studies (Study 38166, Study 20GR142, and Study 20256434), the vaccine candidates were immunogenic.

In Study 38166, male and female rats received 3 weekly IM doses of BNT162b2 up to 100 µg. Serum samples were collected from main study animals on Day 17 (2 days after the third dose) at the end of the dosing phase and on Day 38 at the end of a 3-week recovery phase. The sera were analyzed by ELISA for IgG that bound S1 and RBD as well as for SARS-CoV-2-S pseudovirus neutralizing antibodies. The vaccine candidates elicited IgG that recognized S1 and RBD. After immunization, animals developed high titers of antigen-specific antibodies as well as pseudovirus neutralization titers.

In Study 20GR142, male and female rats received 3 weekly IM doses of up to 100 µg of BNT162b2. Serum samples were collected from study animals prior to vaccine administration, at the end of the dosing phase on Day 17 (2 days after the third dose), and at the end of the 3-week recovery phase on Recovery Phase Day 21. Sera were analyzed for SARS-CoV-2 neutralizing antibodies. After immunization, BNT162b2 elicited SARS-CoV-2 neutralizing antibody responses in males and females at the end of the dosing and recovery phases of the study. SARS-CoV-2 neutralizing antibody responses were not observed in animals prior to vaccine administration or in saline-administered control animals.

In Study 20256434, female rats were administered 30 µg IM doses of BNT162b2 21 and 14 days prior to mating and on GD9 and GD20. Serum samples were collected from females prior to vaccine administration, just prior to mating (M0), at the end of gestation (GD21), and at the end of lactation (LD21) and offspring (fetuses on GD21 and pups on PND21). Sera were analyzed for SARS-CoV-2 neutralizing antibodies. After immunization, SARS-CoV-2 neutralizing titers were detected in all maternal females as well as in their offspring (fetuses and pups). SARS-CoV-2 neutralizing antibody titers were not observed in animals prior to vaccine administration or in saline-administered control animals.

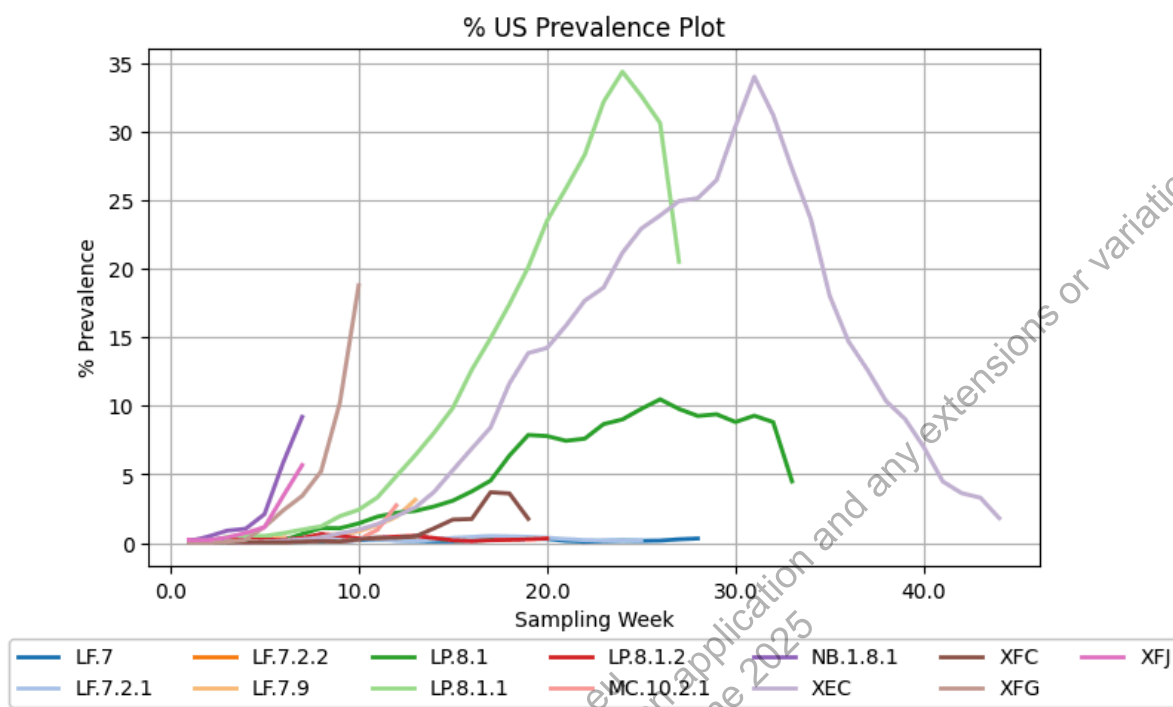
#### 2.4.2.1.6. Variant-Adapted Vaccine Immunogenicity Studies

Over the course of the 2024-2025 season, SARS-CoV-2 has continued to evolve toward new lineages that have remained phylogenetically within the JN.1 lineage cluster but drifted antigenically from earlier JN.1 sublineages through the acquisition of novel combinations of spike amino acid substitutions. At present, JN.1 sublineages (i.e., LP.8.1, XEC, LF.7, XFC, and XFG) continue to cause the majority of SARS-CoV-2 infections in the US and globally (Figure 2.4.2-2). In March 2025, the Omicron LP.8.1 sublineage, a descendent lineage of KP.1.1.3, overtook the recombinant XEC lineage and became the dominant sublineage in the US. Since then, the prevalence of LP.8.1 sublineages has continued to rise to an estimated 40% but has since then subsided to around 35% as of the 2-week period ending 11 May 2025. Recently, XFG lineages (recombinants of LP.8.1 derivatives and LF.7) and LF.7 sublineage have been increasing in prevalence in the US, accounting for over 13% and 5% of cases, respectively (Figure 2.4.2-3). These JN.1 sublineages occupy a unique antigenic space, separate from all other prior Omicron strains (Figure 2.4.2-4). To address this antigenic shift and subsequent antigenic drift from this new lineage cluster, we assessed whether a LP.8.1 variant vaccine update could improve immune responses important to conferring protection from COVID-19 against the currently circulating JN.1 sublineage strains compared to the BNT162b2 KP.2 vaccine. The monovalent BNT162b2 (LP.8.1) vaccine that was tested uses the same mRNA backbone as BNT162b2 and is minimally modified to contain VOC-specific sequence changes of the full-length SARS-CoV-2 P2 S protein that has been evaluated in previous preclinical and clinical studies.

This section summarizes preclinical immunogenicity data for the BNT162b2 monovalent LP.8.1-adapted vaccine compared to the BNT162b2 monovalent KP.2-adapted vaccine.

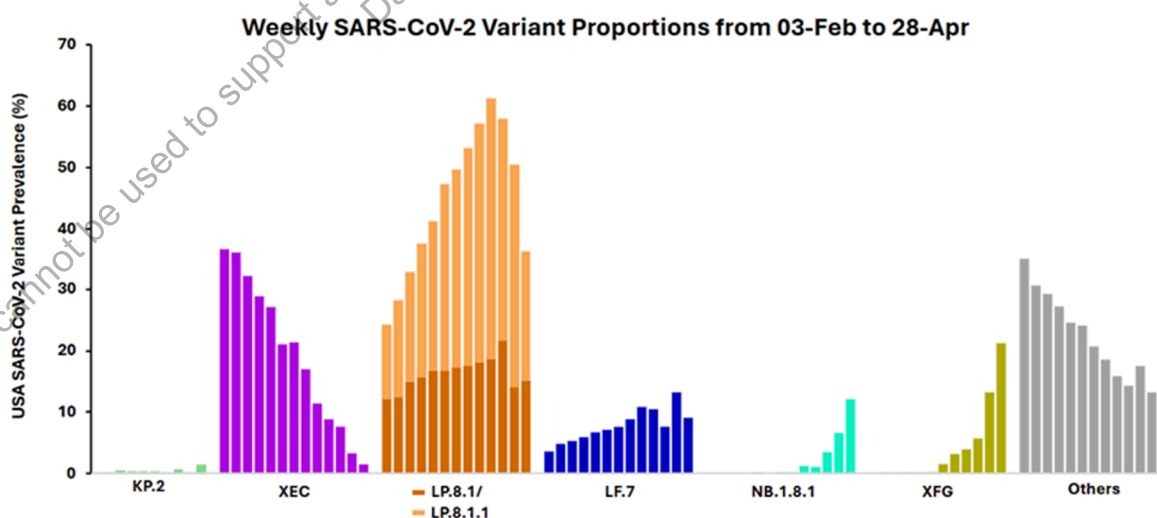


**Figure 2.4.2-2. Epidemiology Trajectories of SARS-CoV-2 JN.1 Sublineages**



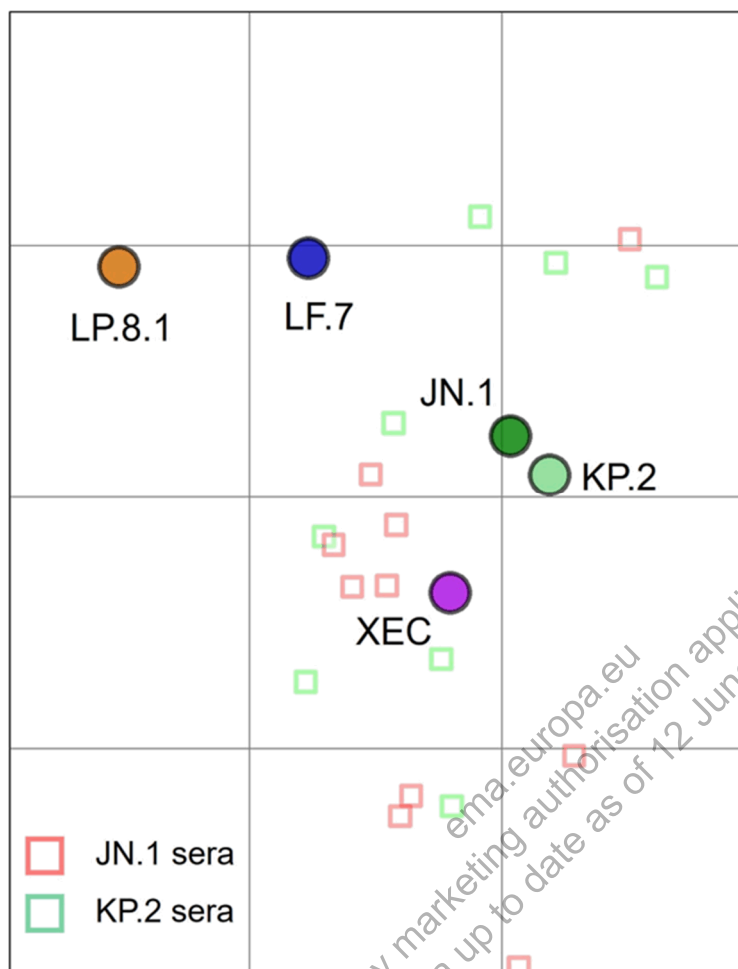
Source: <https://gisaid.org/>; data accessed/analysed/plotted within Pfizer as of 11 May 2025. Labelled lineages are categorized by the same Spike amino acid sequence. Weekly prevalence proportions are then calculated for each lineage group as follows: group weekly count (such as JN.1) \* 100 / total weekly count. The first sampling week notes the earliest week that a lineage group passed 0.1% global prevalence in the GISAID database.

**Figure 2.4.2-3. Global Prevalence Proportions of SARS-CoV-2 Variants**



Source: GISAID - [gisaid.org](https://gisaid.org/); data accessed/analyzed/plotted within Pfizer as of 11 May 2025. Each individual labelled variant includes all subvariants including those with the same Spike protein amino acid sequence. Each bar represents 1 week's variant prevalence data.

**Figure 2.4.2-4. Antigenic Distance of Major SARS-CoV-2 Omicron JN.1 Variants/Subvariants Lineages Assessed in Vaccine Naïve Mice**



This antigenic map represents the relative antigenic distance of SARS-CoV-2 lineages as measured by fold-difference in pseudovirus neutralization titers. Each square on the grid represents a 2-fold difference in neutralization titer assessed from the plasma of mice immunized with the indicated mRNA-vaccine. The antigens are shown in circles and plasma in corresponding color squares. The vaccine regimens used to generate the neutralization data is explained in (VR-VTR-11341); briefly, mice received 2 doses of BNT162b2 JN.1 or KP.2 vaccine. Neutralizing antibody responses against variants of concern pseudovirus panel were measured by pVNT at 1MPD2.

#### 2.4.2.1.6.1. LP.8.1 Variant-Adapted Vaccine

Prior preclinical studies have demonstrated that BNT162b2 variant-adapted vaccines elicit higher neutralizing responses against lineages that are matched or closely matched to that encoded by the vaccine. This trend was observed for the BNT162b2 monovalent Omicron KP.2-adapted vaccine compared to the BNT162b2 XBB.1.5, in both a vaccine-experienced (VR-VTR-11342) and naïve (VR-VTR-11341) mouse model. Subsequent clinical studies demonstrated immunogenicity of the BNT162b2 KP.2-adapted vaccine that closely trended

with the preclinical data. With these historical data predicting clinical performance of the vaccine, preclinical evaluation of the BNT162b2 LP.8.1-adapted vaccine was carried out in a similar manner. A study was performed to assess the immunogenicity of a BNT162b2 LNP-formulated modRNA vaccine candidate encoding the SARS-CoV-2 spike protein of LP.8.1 in BNT162b2-experienced BALB/c mice. The vaccine candidate was evaluated as a monovalent formulation as a fourth dose, compared to the monovalent BNT162b2 KP.2 (VR-VTR-11466). In mice that received 2 doses of BNT162b2 (Original) and 1 dose of bivalent BNT162b2 (Original + BA.4/5), SARS-CoV-2 pseudovirus neutralization tests (pVNT) were performed on sera collected on Day 162 (prior to the fourth dose) and 1 month following administration of the fourth dose with monovalent BNT162b2 KP.2 or LP.8.1. Prior to the fourth dose, all mice exhibited a robust neutralizing antibody response against Wuhan and BA.4/5, and lower neutralizing titers against the antigenically distant JN.1 lineage and sublineages.

At 1 month post Dose 4, the BNT162b2 LP.8 sublineage-modified vaccine elicited 1.8-to-4-fold higher neutralizing responses against XEC, LP.8.1 sublineages (LP.8.1, LP.8.1.1, LP.8.1.2, and LP.8.1.6), MC.10.2.1, NB.1.8.1, and XFG compared to those elicited by the KP.2 vaccine. While the LP.8.1-adapted vaccine immunogenicity against LF.7 and LF.7.2.1 variants was reduced, it remained similar to that of the KP.2-adapted vaccines. Furthermore, the BNT162b2 JN.1 sublineage-modified vaccine induced robust CD4<sup>+</sup> and CD8<sup>+</sup> T cell responses, comparable to those elicited by the KP.2 vaccine. All CD4<sup>+</sup> and CD8<sup>+</sup> T cell responses were highly cross-reactive against Wuhan, BA.4/5, JN.1, KP.2, XEC, and LP.8.1 variants. Together, these data suggest the LP.8.1 modified vaccine improves the immune response against the most predominant circulating SARS-CoV-2 strains.

A separate study was performed to assess the immunogenicity and breadth of neutralization activity of the LP.8.1 vaccine in naïve BALB/c mice as a 2-dose primary series (VR-VTR-11467). The vaccine candidate was evaluated as a monovalent formulation, using current monovalent BNT162b2 KP.2 as a benchmark. SARS-CoV-2 pseudovirus neutralization tests (pVNT) were performed on sera collected on Day 49 (1 month post Dose 2).

The BNT162b2 LP.8.1 vaccine elicited robust neutralizing antibody response that were 2-to-7.7-fold higher against LP.8.1 sublineages (LP.8.1, LP.8.1.1, and LP.8.1.2), XFG, and NB.1.8.1 compared to those elicited by the KP.2-adapted vaccines. LP.8.1-adapted vaccine immunogenicity against LF.7 sub-lineages (LF.7, LF.7.2.1, and LF.7.9) was similar to responses induced with KP.2-adapted vaccines. Furthermore, induced spike specific CD4<sup>+</sup> and CD8<sup>+</sup> T cell cytokine responses were cross-reactive to a broad representation of tested lineages and was comparable to the BNT162b2 KP.2 vaccine. Together, these data suggest that a LP.8.1-adapted vaccine improves the immune response against a broad panel of contemporary and emerging circulating SARS-CoV-2 strains.

#### 2.4.2.2. Secondary Pharmacodynamics

No secondary pharmacodynamics studies were conducted with BNT162b2, or variant vaccines.

**2.4.2.3. Safety Pharmacology**

No safety pharmacology studies were conducted with BNT162b2, or variant vaccines as they are not considered necessary for the development of vaccines according to the WHO guideline ([WHO, 2005](#)).

**2.4.2.4. Pharmacodynamic Drug Interactions**

Nonclinical studies evaluating pharmacodynamic drug interactions with BNT162b2, or variant vaccines were not conducted as they are generally not considered necessary to support development and licensure of vaccine products for infectious diseases (WHO, 2005).

**2.4.2.5. Summary of Nonclinical Pharmacology Findings**

Overall, the nonclinical data demonstrate that the LP.8.1-adapted vaccine, whether administered as booster dose in BNT162b2-experienced mice or as a primary series in naïve mice, elicit the most potent immune responses, against matched or closely matched JN.1 sublineages currently under circulation. T cell responses were cross-reactive to a broad representation of tested lineages and were comparable to the BNT162b2 KP.2 vaccine. The aggregate data demonstrate that a more closely strain-matched vaccine formulation will generate the most potent immune responses that are likely to translate into improved effectiveness. Secondary pharmacodynamics and safety pharmacology studies with BNT162b2 or variant vaccines were not conducted.

### 2.4.3. PHARMACOKINETICS

#### 2.4.3.1. Brief Summary

Assessment of the ADME profile of BNT162b2 (BioNTech code number BNT162, Pfizer code number PF-07302048) included evaluating the PK and metabolism of two novel lipid excipients (ALC-0315 and ALC-0159) in the LNP and potential biodistribution of BNT162b2 using luciferase or GFP mRNA or protein expression as surrogate reporters. An intravenous rat PK study, using LNPs with the identical lipid composition as BNT162b2, demonstrated that ALC-0315 and ALC-0159 distribute from the plasma to the liver. While there was no detectable excretion of either lipid in the urine, the percent of dose excreted unchanged in feces was ~1% for ALC-0315 and ~50% for ALC-0159.

The biodistribution of BNT162b2 was evaluated using luciferase expression as a surrogate reporter in Balb/c mice. Mice were administered a luciferase expressing modRNA formulated like BNT162b2, with the identical lipid composition. Luciferase expression was measured *in vivo* following luciferin application. Luciferase expression was identified at the injection site at 6 hours after injection and was not detected after 9 days. Expression in the liver was also present to a lesser extent at 6 hours after injection and was not detected by 48 hours after injection. The distribution was also examined in male and female Wistar Han rats using LNPs with a comparable lipid composition to BNT162b2 but with a surrogate luciferase mRNA and containing trace amounts of radiolabeled [<sup>3</sup>H]-CHE, a nonexchangeable, nonmetabolizable lipid marker. The greatest mean concentration of LNP was found remaining in the injection site in both sexes. Total recovery (% of injected dose) of LNP outside the injection site was greatest in the liver and was much less in the spleen, adrenal glands, and ovaries. Another study utilizing the luciferase reporter identified the injection site (muscle) and the closest draining lymph node (popliteal) as the main sites of luciferase expression with additional draining lymph nodes on the injection side of the body, liver, and spleen all showing extremely low expression.

The *in vitro* metabolism of ALC-0315 and ALC-0159 was evaluated in blood, liver microsomes, S9 fractions, and hepatocytes from mice, rats, monkeys, and humans. The *in vivo* metabolism was examined in rat plasma, urine, feces, and liver samples from the PK study. Metabolism of ALC-0315 and ALC-0159 appears to occur slowly *in vitro* and *in vivo*. ALC-0315 and ALC-0159 are metabolized by hydrolytic metabolism of the ester and amide functionalities, respectively, and this hydrolytic metabolism is observed across the species evaluated both *in vitro* and *in vivo* for ALC-0315 and *in vitro* only for ALC-0159. No metabolites of ALC-0159 were identified *in vivo*.

The cellular distribution and protein expression of the modRNA-LNP platform of BNT162b2 were evaluated in CD-1 male mice following IM injection of GFP modRNA-LNP. Using IHC and/or ISH, GFP-positive signals were most frequently observed at the injection site in multiple cell types as well as in presumptive leukocytes in the draining and inguinal lymph nodes and spleen, with rare observations in the liver.

Finally, the biodistribution of BNT162b2 mRNA and its translation to spike protein were evaluated in Balb/cJRj mice. The highest ratios of BNT162b2 mRNA containing cells were

in the injected muscle, liver, and spleen at 24 HPD. The lymph nodes also contained mRNA (<1%). Spike protein was detected in the injected muscle and lymph nodes and was not observed in spleen and liver tissue.

#### 2.4.3.2. Methods of Analysis

No methods of analysis have been validated to support GLP TK studies of components of BNT162b2; however, a qualified LC/MS method was developed to support quantitation of the two novel LNP excipients for the non-GLP IV PK study in rats (Study [PF-07302048\\_06Jul20\\_072424](#)).

#### 2.4.3.3. Absorption

##### 2.4.3.3.1. In Vitro Absorption

No absorption studies were conducted for BNT162b2, as the administration route is IM.

##### 2.4.3.3.2. Single-Dose Pharmacokinetics

An intravenous rat PK study (PF-07302048\_06Jul20\_072424; [Tabulated Summary 2.6.5.3](#)) was performed using LNPs containing surrogate luciferase mRNA, with the identical lipid composition as BNT162b2. This study was conducted to explore the disposition of ALC-0315 and ALC-0159 that had reached the systemic circulation following IM administration; thus, the IV route was felt to be appropriate. The findings are depicted in Table 2.4.3-1 and [Figure 2.4.3-1](#).

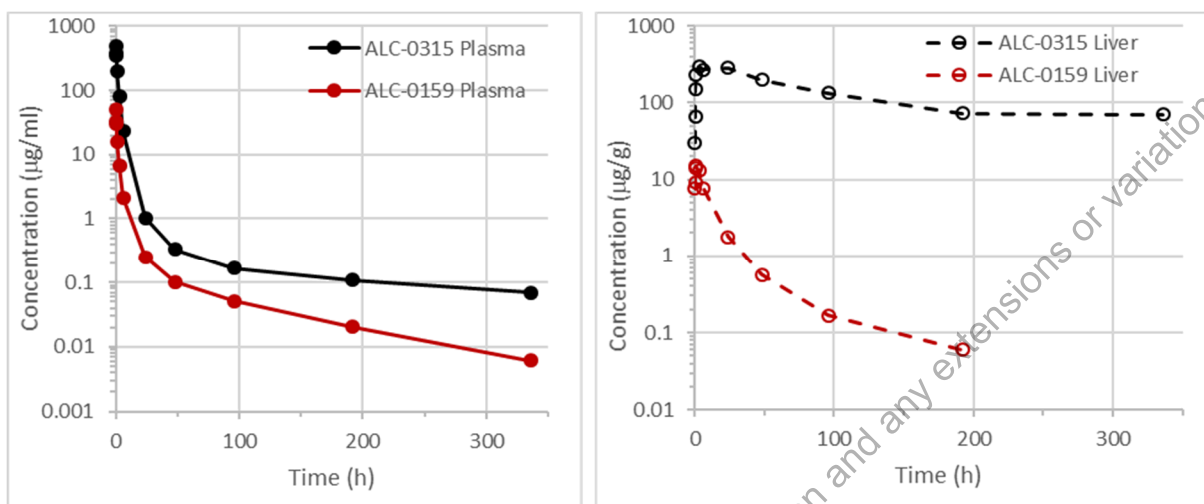
**Table 2.4.3-1. PK of ALC-0315 and ALC-0159 in Wistar Han Rats After IV Administration of LNPs Containing Surrogate Luciferase mRNA at 1 mg/kg**

Analyte	Dose of Analyte (mg/kg)	Gender /N	t <sub>1/2</sub> (h)	AUC <sub>inf</sub> (µg•h/mL)	AUC <sub>last</sub> (µg•h/mL)	Estimated fraction of dose distributed to liver (%) <sup>a</sup>
ALC-0315	15.3	Male/3 <sup>b</sup>	139	1030	1020	60
ALC-0159	1.96	Male/3 <sup>b</sup>	72.7	99.2	98.6	20

a. Calculated as highest mean amount in the liver (µg)/total mean dose (µg) of ALC-0315 or ALC-0159.

b. 3 animals per timepoint; non-serial sampling.

**Figure 2.4.3-1. Plasma and Liver Concentrations of ALC-0315 and ALC-0159 in Wistar Han Rats After IV Administration of LNPs Containing Surrogate Luciferase mRNA at 1 mg/kg**



Pharmacokinetic studies have not been conducted with BNT162b2 and are generally not considered necessary to support the development and licensure of vaccine products for infectious diseases (WHO, 2005; WHO, 2014).

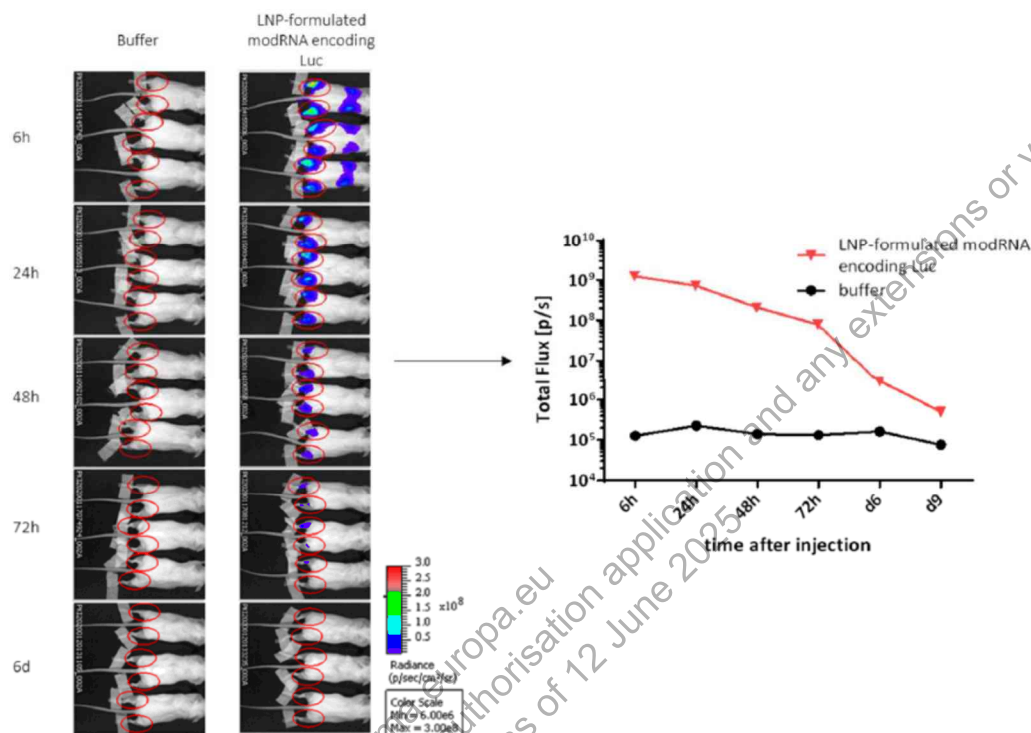
#### 2.4.3.4. Distribution

In an in vivo study (R-20-0072; Tabulated Summary 2.6.5.5A), biodistribution was assessed using luciferase as a surrogate marker protein, with modRNA encoding luciferase formulated like BNT162b2, with the identical lipid composition. The LNP-formulated luciferase-encoding modRNA was administered to Balb/c mice by IM injection of 1 µg each in the right and left hind leg (for a total of 2 µg). Using in vivo bioluminescence after injection of luciferin substrate, luciferase protein expression was detected at different timepoints at the site of injection and to a lesser extent, and more transiently, in the liver (Figure 2.4.3-2). Distribution to the liver is likely mediated by LNPs entering the blood stream. The luciferase expression at the injection sites dropped to background levels after 9 days. The repeat-dose toxicity study in rats showed no evidence of liver injury (Section 2.4.4.3).

The biodistribution of the antigen encoded by the modRNA component of BNT162b2 is expected to be dependent on the LNP distribution and the results presented should be representative for the vaccine mRNA platform, as the LNP-formulated luciferase-encoding modRNA had the same lipid composition.



**Figure 2.4.3-2. Bioluminescence Emission in Balb/c Mice after IM Injection of an LNP Formulation of modRNA Encoding Luciferase**



The distribution of a LNP with a comparable lipid composition to BNT162b2 but with a surrogate luciferase mRNA (monitoring the <sup>3</sup>H-CHE lipid label), was investigated in blood, plasma and selected tissues in male and female Wistar Han rats over 48 hours after a single IM injection at 50 µg mRNA/animal (Study 185350; Tabulated Summary 2.6.5.5B). The greatest mean concentration of LNP was found remaining in the injection site at each time point in both sexes. Outside the injection site, low levels of radioactivity were detected in most tissues, with the greatest levels in plasma observed 1-4 HPD. Over 48 hours, the LNP distributed mainly to liver, adrenal glands, spleen and ovaries, with maximum concentrations observed at 8-48 HPD. Total recovery (% of injected dose) of LNP, for combined male and female animals, outside of the injection site was greatest in the liver (up to 18%) and was much less in the spleen (≤1.0%), adrenal glands (≤0.11%) and ovaries (≤0.095%). The mean concentrations and tissue distribution pattern were broadly similar between the sexes.

An in vivo study evaluated the biodistribution of LNP-formulated modRNA encoding luciferase, using the same modRNA-LNP platform as BNT162b2, in Balb/c mice (Study R-23-0355; Tabulated Summary 2.6.5.5C). Following IM administration of 0.2 µg or 1.0 µg modRNA-LNP, animals were evaluated by in vivo BLI and tissues were evaluated for luciferase expression. Total luciferase expression in all organs of animals that received 1.0 µg modRNA-LNP showed statistically significant higher luciferase expression 24 HPD compared with Day 6.



The injection site (muscle) and the closest draining lymph node (popliteal) were the main sites of luciferase expression for both modRNA-LNP dose levels, while additional draining lymph nodes on the right side of the body (where the injection was given), liver, and spleen all showed extremely low expression. At both dose levels, mRNA was distributed to the same main target organs, but the higher dose led to an increase in luciferase expression in lymph node tissue, suggesting potential influence of the modRNA dose on lymphatic drainage. BLI analysis also showed luciferase expression decreasing from Day 1 to Day 6 with the signal being detected mainly at the injection site.

To better understand the cellular distribution and protein expression of the modRNA-LNP platform of BNT162b2 in select tissues, a time course study was conducted in CD-1 male mice following IM injection of 1 µg each in the right and left quadricep muscle (for a total of 2 µg) of GFP modRNA-LNP (Study 22GR161; [Tabulated Summary 2.6.5.16](#)). IHC identified cells that had taken up the modRNA-LNP and translated the mRNA to GFP, while ISH localized GFP mRNA in cells that had internalized the GFP modRNA-LNP.

GFP detected in the serum peaked at 6 HPD and gradually declined through 168 HPD. Using IHC (for protein) and ISH (for mRNA) methods, GFP mRNA and protein distribution was similar to that observed in the other biodistribution studies and was most frequent at the injection site, in the draining and inguinal lymph nodes, and spleen, with rare observations in the liver. GFP-positive signals were consistently detected in multiple cell types at the injection site: adipocytes, endothelium and perivascular connective tissue from thin-walled vessels (presumptive venules, capillaries, lymphatics), dermal fibroblasts, muscle connective tissues (epimysium, perimysium, and endomysium), rare myocytes, and mononuclear cells, as well as presumptive leukocytes in lymph nodes and spleen, and hepatocytes (for RNA only at 6 HPD). In muscle compartments in the injection site, GFP-positive signals were generally greatest at 6 and 24 HPD except in myocytes where the highest incidence occurred at 168 HPD. GFP-positive staining was not observed in the heart by either method.

IHC (for protein) and ISH (for mRNA) staining generally overlapped; although, in spleen and liver, GFP-positive staining was only detectable by ISH and in inguinal lymph nodes, ISH labeling was present in multiple animals across time points but IHC labeling was only observed in 2 animals. Electron microscopy detected structures consistent with LNPs in spleen samples at 24 and 72 HPD, but not at 6 HPD; structures were not detected in the draining lymph nodes or injection site muscle samples.

Additionally, the biodistribution of BNT162b2 mRNA and its translation to spike protein in Balb/cJrj mice were evaluated (Study [R-23-0475](#); [Tabulated Summary 2.6.5.5D](#)). Following IM administration of 1 µg BNT162b2 in the right hind muscle, organs were collected 24 HPD for analysis. The highest ratios of BNT162b2 mRNA containing cells were in the injected muscle (2.1% to 15.9%), liver (3% to 8%), and spleen (1.4% to 3.8%) at 24 HPD. The mRNA was also present (<1%) in inguinal, popliteal, and axillary lymph nodes. Tissues from heart and lung showed ratios of BNT162b2 mRNA containing cells comparable to the saline control. For the brain, no conclusion could be drawn due to non-specific binding of the probe used for BNT162b2 mRNA detection.

IHC-based analysis revealed the presence of spike protein in the injected muscle (with mean ratios of positive cells from 11% to 16%), and popliteal and inguinal lymph nodes (with mean ratios of positive areas from 0.3% to 1.7% and 0 to 1.6%, respectively) of all BNT162b2-injected mice. In one of the three mice, the axillary lymph node was also positive for spike protein expression with a mean positive area of 4%. There was no definitive evidence of spike expression in the brain, spleen, liver, lung, and heart.

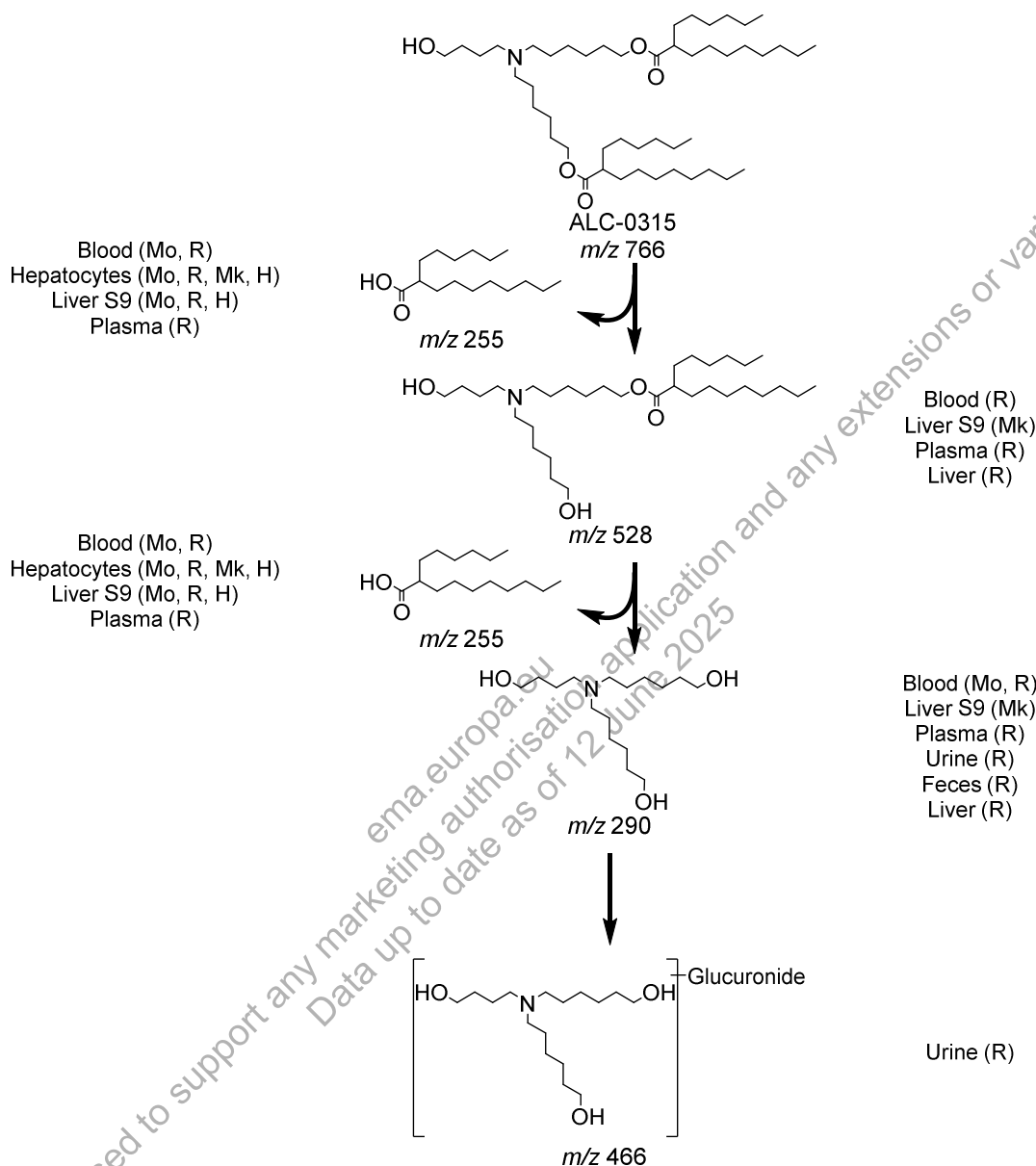
BNT162b2 mRNA was not translated into the spike protein in all cell types to which it was distributed. Translation appears to happen in several cell types in the muscle. In the lymph nodes, most of the cells expressing spike protein appeared to be macrophages. In contrast, cells located in the germinal centers, which were also positive for BNT162b2 mRNA, did not express spike protein. In the spleen, vaccine mRNA was restricted to the white pulp areas, which were strictly negative for spike protein. Finally, in the liver tissue, BNT162b2 mRNA appeared homogeneously distributed with no detectable translation into spike protein.

#### 2.4.3.5. Metabolism

Of the four lipids used as excipients in the LNP formulation, two are naturally occurring (cholesterol and DSPC) and will be metabolized and excreted like their endogenous counterparts. The *in vitro* metabolic stability of the two novel lipids, ALC-0315 (aminolipid) and ALC-0159 (PEG-lipid), were evaluated in mouse, rat, monkey, and human liver microsomes, S9 fractions, and hepatocytes. ALC-0315 and ALC-0159 were stable (>82% remaining) over 120 min in liver microsomes and S9 fractions and over 240 min in hepatocytes in all species and test systems (Studies 01049-20008, 01049-20009, 01049-20010, 01049-20020, 01049-20021, and 01049-20022; Tabulated Summaries 2.6.5.10A and 2.6.5.10B).

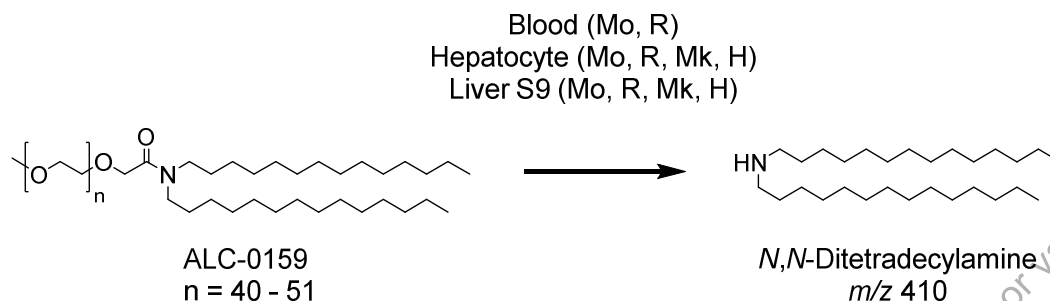
Further study of the metabolism of ALC-0315 and ALC-0159 *in vitro* and *in vivo* evaluating the plasma, urine, feces, and liver from the rat PK study (Section 2.4.3.3.2) determined ALC-0315 and ALC-0159 are metabolized slowly (Study PF-07302048\_05Aug20\_043725; Tabulated Summaries 2.6.5.9, 2.6.5.10C, and 2.6.5.10D). ALC-0315 and ALC-0159 underwent hydrolytic metabolism of the ester and amide functionalities, respectively, and this hydrolytic metabolism was observed across the species evaluated both *in vitro* and *in vivo* for ALC-0315 and *in vitro* only for ALC-0159 (Figure 2.4.3-3 and Figure 2.4.3-4). No metabolites of ALC-0159 were identified *in vivo*.

**Figure 2.4.3-3. Proposed Biotransformation Pathway of ALC-0315 in Various Species**



Metabolism of ALC-0315 occurs via two sequential ester hydrolysis reactions, first yielding the monoester metabolite ( $m/z$  528) followed by the doubly deesterified metabolite ( $m/z$  290). Subsequent metabolism of the doubly deesterified metabolite resulted in a glucuronide metabolite ( $m/z$  466), which was only observed in urine from the rat PK study. Additionally, 6-hexyldecanoic acid ( $m/z$  255), the acid product of both hydrolysis reactions of ALC-0315, was identified.

**Figure 2.4.3-4. Proposed Biotransformation Pathway of ALC-0159 in Various Species**



The primary route of metabolism identified for ALC-0159 involves amide bond hydrolysis yielding *N,N*-ditetradecylamine ( $m/z$  410).

The protein encoded by the modRNA in BNT162b2 is expected to be proteolytically degraded like other endogenous proteins. RNA is degraded by cellular RNases and subjected to nucleic acid metabolism. Nucleotide metabolism occurs continuously within the cell, with the nucleoside being degraded to waste products and excreted or recycled for nucleotide synthesis. Therefore, no RNA or protein metabolism or excretion studies will be conducted.

#### 2.4.3.6. Excretion

In the rat PK study ([Section 2.4.3.3.2](#)), there was no detectable excretion of ALC-0315 and ALC-0159 in urine after IV administration of LNPs containing surrogate luciferase RNA at 1 mg/kg. The percent excreted unchanged in feces was ~1% for ALC-0315 and ~50% for ALC-0159. Metabolites of ALC-0315 were detected in the urine of rats ([Figure 2.4.3-3](#)). No excretion studies have been conducted with BNT162b2 for the reasons described in [Section 2.4.3.5](#).

#### 2.4.3.7. Pharmacokinetic Drug Interactions

No PK drug interaction studies have been conducted with BNT162b2.

## 2.4.4. TOXICOLOGY

### 2.4.4.1. Brief Summary

The nonclinical safety of the BNT162 modRNA-LNP platform has been well-characterized in the SARS-CoV-2 vaccine program, which included 2 GLP-compliant repeat-dose toxicity studies and a GLP-compliant DART study in Wistar Han rats, as outlined in Table 2.4.4-1. The BNT162b2 vaccine was also evaluated in a DART study (Bowman et al, 2021). Nonclinical safety of the modRNA-LNP platform is further validated by repeat-dose toxicity and DART studies of two additional, highly similar BNT162 modRNA vaccine candidates (BNT162b1 and/or BNT162b3; Rohde et al, 2023). The platform approach is justified for mRNA-based vaccines based on the WHO guidance (WHO, 2022).

**Table 2.4.4-1. Overview of Toxicity Testing Program of BNT162 Vaccines Using modRNA-LNP Platform**

Study	Study (Sponsor Reference Number)	Group/ Dose, µg RNA	Number of Animals	GLP <sup>a</sup>
<b>Repeat-Dose Toxicity</b>				
17-Day, QW, IM Toxicity With 3 Week Recovery in Rats	38166	Control <sup>b</sup> , 0 BNT162b1, 30 & 100 BNT162b2, 100	15/sex 15/sex/dose 15/sex	Yes
17-Day, QW, IM Toxicity With 3 Week Recovery in Rats	20GR142	Saline <sup>c</sup> , 0 BNT162b2, 30 BNT162b3, 30	15/sex 15/sex 15/sex	Yes
<b>Developmental and Reproductive Toxicity</b>				
Combined Fertility and Developmental Study (Including Teratogenicity and Postnatal Investigations) in Rats	20256434 (RN9391R58)	Saline <sup>c</sup> , 0 BNT162b1, 30 BNT162b2, 30 BNT162b3, 30	44 F 44 F 44 F 44 F	Yes

a. All GLP studies were conducted in an OECD mutual acceptance of data (MAD) compliant member state.

b. Phosphate buffered saline, 300 mM sucrose.

c. Sterile saline (0.9% NaCl).

In the toxicity studies, once-a-week IM administrations of BNT162b1, BNT162b2, or BNT162b3 for a total of 3 doses were tolerated with no evidence of systemic toxicities. Expected inflammatory responses to the vaccine were observed, such as erythema and edema at the injection sites, body temperature increases, elevations in WBCs and acute phase reactants, lower A:G ratios, enlarged draining iliac lymph nodes and spleen, and microscopic inflammation at injection sites and surrounding tissues as well as increased cellularity in the draining (iliac) lymph nodes, bone marrow, and spleen.

In the DART study, IM administration of BNT162b1, BNT162b2, or BNT162b3 to female rats twice before the start of mating and twice during gestation at the human clinical dose (30 µg RNA/dosing day) showed no effects on mating performance, fertility, or any ovarian or uterine parameters in the F0 female rats or on embryo-fetal or postnatal survival, growth, or development in the F1 offspring through the end of lactation. A SARS-CoV-2 neutralizing antibody response to each vaccine was confirmed in F0 female rats prior to mating, at the end

of gestation, and at the end of lactation. The neutralizing antibodies were also detectable in the F1 offspring (fetuses and pups).

#### 2.4.4.2. Single-Dose Toxicity

A separate single-dose toxicity study with BNT162b2 has not been conducted.

#### 2.4.4.3. Repeat-Dose Toxicity

No repeat-dose toxicity studies have been conducted with BNT162b2 variant vaccines. Repeat-dose toxicity studies of the BNT162 modRNA vaccine candidates supporting platform safety are summarized below.

Two 17-day GLP-compliant IM toxicity studies in Wistar Han rats (Studies 38166; [Tabulated Summary 2.6.7.7A](#) and 20GR142; [Tabulated Summary 2.6.7.7B](#)) were conducted to evaluate BNT162b2 as well as other BNT162 modRNA vaccine candidates (BNT162b1 up to 100 µg and BNT162b3 at 30 µg, respectively). In both studies, the findings were similar and generally consistent with those associated with the IM administration of LNP-encapsulated mRNA vaccines ([Hassett et al, 2019](#)).

All BNT162 vaccine candidates tested were tolerated without evidence of systemic toxicities. Expected inflammatory responses to the vaccine were evident such as edema and erythema at the injection sites, transient elevation in body temperature, elevations in WBCs and acute phase reactants, and lower A:G ratios. Injection site reactions were common in vaccine-administered animals and were greater after boost immunizations. Changes secondary to inflammation included slight and transient reductions in body weight and transient reductions in RETIC, PLT, and RBC mass parameters. All changes noted in the dosing phase were reversible except for higher RDW, higher globulins, and/or lower A:G ratios in animals administered BNT162b2 (V9) or BNT162b3. The higher RDW reflects prior reticulocyte increases which occurred as a regenerative response to reticulocyte decreases observed during dosing. The lower A:G ratio was due to higher globulins, which is an expected immune response to vaccine administration ([Sellers et al, 2020](#)). A robust SARS-CoV-2 S-specific antibody response was elicited to all BNT162 encoded antigens in both studies.

Macroscopic pathology and organ weight changes were also consistent with immune activation and inflammatory response and included increased size of draining iliac lymph nodes, and increased size and weight of spleen. Vaccine-related microscopic findings at the end of the dosing phase consisted of edema and inflammation in injection sites and surrounding tissues; increased cellularity in the draining (iliac) and inguinal lymph nodes, bone marrow, and spleen.

Periportal vacuolation of hepatocytes was observed in both studies and was not associated with microscopic or biochemical evidence of hepatocyte damage and was considered to reflect hepatocyte uptake of the lipids from the LNP formulation ([Kozauer et al, 2018](#)). A transient elevation in GGT was noted in animals vaccinated with BNT162b1 or BNT162b2 in Study 38166 without evidence of microscopic changes in the biliary system or other



hepatobiliary biomarkers and was not recapitulated in Study 20GR142. Elevated GGT was not attributed to the hepatocyte vacuolation.

#### 2.4.4.4. Genotoxicity

No genotoxicity studies are planned for BNT162b2, or variant vaccines as the components of the vaccine construct are lipids and RNA and are not expected to have genotoxic potential (WHO, 2005).

#### 2.4.4.5. Carcinogenicity

Carcinogenicity studies with BNT162b2, or variant vaccines have not been conducted as the components of the vaccine construct are lipids and RNA and are not expected to have carcinogenic or tumorigenic potential. Carcinogenicity testing is generally not considered necessary to support the development and licensure of vaccine products for infectious diseases (WHO, 2005).

#### 2.4.4.6. Reproductive and Developmental Toxicity

No DART studies have been conducted with the BNT162b2 variant vaccines. DART studies conducted with the BNT162 modRNA vaccine candidates supporting the platform safety are summarized below.

Macroscopic and microscopic evaluation of male and female reproductive tissues from the repeat-dose toxicity studies (Section 2.4.4.3) with BNT162b1, BNT162b2 (V8 or V9) or BNT162b3 showed no evidence of toxicity.

Reproductive and developmental toxicity assessments were made using the BNT162b1, BNT162b2, and BNT162b3 (Study 20256434; Tabulated Summary 2.6.7.12) vaccine candidates. IM injections of the vaccine to female rats (F0) twice before the start of mating and twice during gestation at the human clinical dose (30 µg) had no effects on mating performance, fertility, or any ovarian or uterine parameters in the F0 female rats nor on embryo-fetal or postnatal survival, growth, or development in the F1 offspring. An immune response was confirmed in F0 female rats following administration of each vaccine candidate and these responses were also detectable in the F1 offspring (fetuses and pups).

#### 2.4.4.7. Local Tolerance

Local tolerance of IM administration of BNT162b2 was evaluated by injection site observations and macroscopic and microscopic examination of injection sites in the repeat-dose toxicity studies and is described in Section 2.4.4.3.

#### 2.4.4.8. Other Toxicity Studies

##### 2.4.4.8.1. Phototoxicity

Phototoxicity studies with BNT162b2, or variant vaccines have not been conducted.

#### **2.4.4.8.2. Antigenicity**

Immunogenicity was evaluated as part of the primary pharmacodynamic studies (Section 2.4.2.1). Serology data from the repeat-dose toxicity studies shows a robust antigen-specific immune response to BNT162b2.

#### **2.4.4.8.3. Immunotoxicity**

Stand-alone immunotoxicity studies with BNT162b2, or variant vaccines have not been conducted. However, immunotoxicological endpoints were collected as part of the repeat-dose toxicity studies; there were no adverse effects observed and no significant effects on measured cytokines.

#### **2.4.4.8.4. Mechanistic Studies**

Mechanistic studies with BNT162b2, or variant vaccines have not been conducted.

#### **2.4.4.8.5. Dependence**

Dependence studies with BNT162b2, or variant vaccines have not been conducted.

#### **2.4.4.8.6. Studies on Metabolites**

Stand-alone studies with administration of metabolites of BNT162b2, or variant vaccines have not been conducted.

#### **2.4.4.8.7. Studies on Impurities**

Stand-alone studies with administration of impurities of BNT162b2, or variant vaccines have not been conducted.

#### **2.4.4.8.8. Other Studies**

No other studies with BNT162b2, or variant vaccines evaluated in this submission have been conducted.

#### **2.4.4.9. Discussion of Findings**

No nonclinical safety studies have been conducted with the BNT162b2 variant vaccines. Based on the nonclinical experience with 4 BNT162 candidates (BNT162b1, BNT162b2, and BNT162b3) that utilized the same RNA-LNP platform, target organs identified were the injection site, draining (iliac) and inguinal lymph nodes, spleen, bone marrow, and liver in rats for this modality. All findings were nonadverse and reversible. Injection site findings included transient erythema and edema and microscopic mixed cell inflammation with edema. Periportal vacuolation of hepatocytes was observed in both studies and was considered to reflect hepatocyte uptake of the lipids from the LNP formulation (Kozauer et al, 2018). Immune organ effects included macroscopic enlargement of the draining and regional lymph nodes correlating microscopically to increased germinal center cellularity and increased plasma cells; increased spleen weights correlating to germinal center cellularity



and increased hematopoiesis; and increased bone marrow hematopoiesis. All immune organ effects were the result of immune stimulation and/or inflammation associated with vaccine.

090177e1a339ef23a\Approved\Approved On: 23-May-2025 19:18 (GMT)

### 2.4.5. INTEGRATED OVERVIEW AND CONCLUSIONS

The nonclinical program demonstrates that BNT162b2 is immunogenic in mice, rats, and nonhuman primates, and the toxicity studies support the licensure of this vaccine. Preclinical assessments in mice and nonhuman primates demonstrate that BNT162b2 elicits a rapid antibody response with measurable SARS-CoV-2 neutralizing titers after a single dose and substantial increases in titers after a second dose that exceed titers in sera from SARS-CoV-2/COVID-19-recovered patients. A Th1-dominant T cell response was evident in both mice and nonhuman primates. In a SARS-CoV-2 rhesus challenge model, BNT162b2 provided complete protection in the lungs, as determined by lack of detectable viral RNA, and there was no evidence of vaccine-elicited disease enhancement.

Variant-adapted BNT162b2 Omicron KP.2 evaluated as a fourth dose against a background series of 2 doses of BNT162b2 (Original) and 1 dose of bivalent BNT162b2 (Original + BA.4/5), previously was shown to elicit robust neutralizing antibody responses in mice, as compared to a fourth dose booster of XBB.1.5 vaccine. Responses were highest against the matched KP.2 or closely related JN.1 sublineages. When administered as a primary vaccination series to immunologically naïve mice, the KP.2 vaccine generated neutralizing antibody responses against matched or closely matched JN.1 sublineage pseudoviruses that far exceeded those elicited by the XBB.1.5 vaccine.

The newly developed BNT162b2 Omicron LP.8.1-adapted vaccine was evaluated as a fourth dose against a background series of 2 doses of BNT162b2 (Original) and 1 dose of bivalent BNT162b2 (Original + BA.4/5) to better approximate the general population immunity. A fourth dose of KP.2-adapted vaccine was used as a comparator. The LP.8.1-adapted vaccine elicited 1.8-to-4-fold higher neutralizing antibody responses than the KP.2 vaccine against LP.8.1 sublineage strains that harbor amino acid changes associated with greater immune escape potential. While the LP.8.1-adapted vaccine's immunogenicity against LF.7 and LF.7.2.1 variants of JN.1 lineage was reduced, it remained similar to that of the KP.2-adapted vaccines. These same trends held for the primary series study with an even greater magnitude of difference between the LP.8.1 and KP.2 vaccine against all tested LP.8.1 sublineage strains. Furthermore, the LP.8.1 vaccine induced robust CD4<sup>+</sup> and CD8<sup>+</sup> T cell responses, not only against LP.8.1 but also against the KP.2 and XEC strains of the JN.1 sublineage. Together, these data suggest that the LP.8.1 lineage-modified vaccine improves the immune response against the most predominant currently circulating SARS-CoV-2 strains.

There were no ADME studies conducted with the BNT162b2 variants. An IV rat PK study, using an LNP with the identical lipid composition as BNT162b2, demonstrated that the novel lipid excipients, ALC-0315 and ALC-0159, distribute from the plasma to the liver. While there was no detectable excretion of either lipid in the urine, the percent of dose excreted unchanged in feces was ~1% for ALC-0315 and ~50% for ALC-0159. Further studies indicated metabolism played a role in the elimination of ALC-0315. Metabolism of ALC-0315 and ALC-0159 appears to occur slowly in vitro and in vivo in nonclinical species. ALC-0315 and ALC-0159 are metabolized by hydrolytic metabolism of the ester and amide functionalities, respectively, and this hydrolytic metabolism was observed across the species

evaluated both in vitro and in vivo for ALC-0315 and in vitro only for ALC-0159. No metabolites of ALC-0159 were identified in vivo.

Biodistribution was initially assessed using luciferase or GFP expression as surrogate reporters formulated like BNT162b2, with the identical lipid composition, or using a radiolabeled LNP-mRNA formulation. After IM injection of the modRNA-LNPs in mice, luciferase or GFP protein expression was mainly demonstrated at the site of injection and the draining lymph nodes. Following IM administration of a radiolabeled LNP-mRNA formulation to rats, the percent of dose was also greatest at the injection site with total recovery of radioactivity next greatest in the liver and much lower in the spleen, adrenal glands, and ovaries.

In mice that were administered BNT162b2, the highest ratios of BNT162b2 mRNA containing cells were in the injected muscle, liver, and spleen at 24 HPD with the lymph nodes also containing mRNA. Spike protein was detected in the injected muscle and lymph nodes and not observed in spleen and liver tissue.

There were no toxicity studies conducted with the BNT162b2 variants. Administration of BNT162b2 by IM injection to male and female Wistar Han rats once every week for a total of 3 weekly cycles of dosing was tolerated without evidence of systemic toxicity in GLP-compliant repeat-dose toxicity studies. For BNT162b2, expected immune responses to the vaccine were evident, such as edema and erythema at the injection sites, transient elevation in body temperature, elevations in WBCs and acute phase reactants, and decreased A:G ratios. Injection site reactions were common in all vaccine-administered animals and were greater after boost immunizations. Changes secondary to inflammation included slight and transient reductions in body weights and transient reductions in RETIC, PLT, and RBC mass parameters. All changes in hematology parameters and acute phase proteins were similar to control at the end of the recovery phase for BNT162b2 with the exception of higher RDW and lower A:G ratios in animals administered BNT162b2. Macroscopic pathology and organ weight changes were also consistent with immune activation and inflammatory response and included increased size of draining iliac lymph nodes and increased size and weight of spleen. Vaccine-related microscopic findings at the end of dosing for BNT162b2 were evident in injection sites and surrounding tissues, in the draining iliac lymph nodes, bone marrow, spleen, and liver. Microscopic findings at the end of the dosing phase were partially (recovery in progress) or completely recovered in all animals at the end of the recovery phase for BNT162b2. A robust immune response was elicited to the BNT162b2 vaccine antigen. These studies also evaluated additional BNT162 vaccine candidates, and the results were similar across the variants.

Administration of BNT162b2 to female rats twice before the start of mating and twice during gestation at the human clinical dose (30 µg RNA/dosing day) was associated with nonadverse effects (body weight, food consumption, and effects localized to the injection site) after each dose administration. There were no effects of BNT162b2 administration on mating performance, fertility, or any ovarian or uterine parameters in the F0 female rats nor on embryo-fetal or postnatal survival, growth, or development in the F1 offspring. An immune response was confirmed in F0 female rats following administration of BNT162b2 and this response was also detectable in the F1 offspring (fetuses and pups).

In conclusion, the nonclinical package of BNT162b2 supports the updates to licensing and marketing applications of a BNT162b2 variant vaccine, which uses the same LNP platform.

090177e1a39ef23a\Approved\Approved On: 23-May-2025 19:18 (GMT)

CONFIDENTIAL

#### 2.4.6. LIST OF LITERATURE REFERENCES

Bowman CJ, Bouressam M, Campion S, et al. Lack of effects on female fertility and prenatal and postnatal offspring development in rats with BNT162b2, a mRNA-based COVID-19 vaccine. *Reproductive Toxicology*. 2021;103:28-35.

Cai Y, Zhang J, Xiao T, et al. Distinct conformational states of SARS-CoV-2 spike protein. *Science*. 2020;10.1126/science.abd4251.

Hassett KJ, Benenato KE, Jacquinet E, et al. Optimization of Lipid Nanoparticles for Intramuscular Administration of mRNA Vaccines. *Mol Ther Nucleic Acids*. 2019;15:1-11.

Jiang S, Hyllier C, Du L. Neutralizing antibodies against SARS-CoV-2 and other human coronaviruses. *Science and Society. Trends Immunol*. 2020;41(5)(May):355-9.

Ke Z, Oton J, Qu K, et al. Structures and distributions of SARS-CoV-2 spike protein trimers on intact virions. *Nature*. 2020;588:498-502.

Kim JY, Ko JH, Kim Y, et al. Viral load kinetics of SARS-CoV-2 infection in first two patients in Korea. *J Korean Med Sci*. 2020;35(7)(Feb):e86.

Kozauer NA, Dunn WH, Unger EF, et al. CBER multi-discipline review of Onpattro. NDA 210922. 10 Aug 2018.

Munster VJ, Feldmann F, Williamson BN, et al. Respiratory disease in rhesus macaques inoculated with SARS-CoV-2. *Nature*. 2020;585:268-72.

Pallesen J, Wang N, Corbett KS, et al. Immunogenicity and structures of a rationally designed prefusion MERS-CoV spike antigen. *Proc Natl Acad Sci USA*. 2017;114(35):E7348-57.

Pardi N, Hogan MJ, Pelc RS, et al. Zika virus protection by a single low-dose nucleoside-modified mRNA vaccination. *Nature*. 2017;543(7644):248-51.

Pardi N, Parkhouse K, Kirkpatrick E, et al. Nucleoside-modified mRNA immunization elicits influenza virus hemagglutinin stalk-specific antibodies. *Nat Comm*. 2018;9(1)(08):3361.

Rohde CM, Lindemann C, Giovanelli M, et al. Toxicological assessments of a pandemic COVID-19 vaccine - demonstrating the suitability of a platform approach for mRNA vaccines. *Vaccines*. 2023;11(2):417.

Sahin U, Karikó K, Türeci Ö. mRNA-based therapeutics - developing a new class of drugs. *Nat Rev Drug Discov*. 2014;13(10):759-80.

Sellers RS, Nelson K, Bennet B, et al. Scientific and regulatory policy committee points to consider\*: approaches to the conduct and interpretation of vaccine safety studies for clinical and anatomic pathologists. *Toxicol Pathol*. 2020;48(2):257-76.

Singh DK, Singh B, Ganatra SR, et al. Responses to acute infection with SARS-CoV-2 in the lungs of rhesus macaques, baboons and marmosets. *Nat Microbiol.* 2021;6:73-86.

US Department of Health and Human Services, Food and Drug Administration, Center for Biologics Evaluation and Research. Development and licensure of vaccines to prevent COVID-19. In: Guidance for industry. Rockville, MD: Food and Drug Administration; 2020: 21 pages.

World Health Organization. WHO guidelines on nonclinical evaluation of vaccines. Annex 1. In: World Health Organization. WHO technical report series, no. 927. Geneva, Switzerland; World Health Organization. 2005:31-63.

World Health Organization. Annex 2. Guidelines on the nonclinical evaluation of vaccine adjuvants and adjuvanted vaccines. In: WHO technical report series no. 987. Geneva, Switzerland: World Health Organization. 2014:59-100.

WHO. Annex 3. Evaluation of the quality, safety and efficacy of messenger RNA vaccines for the prevention of infectious diseases: regulatory considerations, In: Technical Report Series No 1039. Geneva Switzerland. World Health Organization (WHO); 2022: p. 88-154.

Wrapp D, Wang N, Corbett KS, et al. Cryo-EM structure of the 2019-nCoV spike in the prefusion conformation. *Science.* 2020;367(6483):1260-3.

Yong CY, Ong HK, Yeap SK, et al. Recent advances in the vaccine development against middle east respiratory syndrome-coronavirus. *Front Microbiol.* 2019;10:1781.

Zakhartchouk AN, Sharon C, Satkunarajah M, et al. Immunogenicity of a receptor-binding domain of SARS coronavirus spike protein in mice: implications for a subunit vaccine. *Vaccine.* 2007;25(1):136-43.

Zost S, Gilchuk P, Chen R, et al. Rapid isolation and profiling of a diverse panel of human monoclonal antibodies targeting the SARS-CoV-2 spike protein. *Nat Med.* 2020;26:1422-7.

Zou L, Ruan F, Huang M, et al. SARS-CoV-2 viral load in upper respiratory specimens of infected patients. *N Engl J Med.* 2020;382(12)(03):1177-9.